Liquid polymorphism: water in nanoconfined and biological environments

2010 J. Phys.: Condens. Matter 22 284101

(http://iopscience.iop.org/0953-8984/22/28/284101)

J. Phys.: Condens. Matter **22** (2010) 284101 (12pp) doi:10.1088/0953-8984/22/28/284101

Liquid polymorphism: water in nanoconfined and biological environments

H E Stanley[1], S V Buldyrev[2], G Franzese[1,3], P Kumar[1], F Mallamace[4], M G Mazza[1], K Stokely[1] and L Xu[5]

[1] Center for Polymer Studies and Department of Physics, Boston University, Boston, MA 02215, USA
[2] Department of Physics, Yeshiva University, 500 West 185th Street, New York, NY 10033, USA
[3] Departament de Física Fonamental, Universitat de Barcelona, Diagonal 647, Barcelona 08028, Spain
[4] Dipartimento di Fisica, Universita di Messina, Vill. S Agata, CP 55, I-98166 Messina, Italy
[5] World Premier International (WPI) Research Center, Advanced Institute for Materials Research, Tohoku University, Sendai 980-8577, Japan

Received 16 April 2010
Published 21 June 2010
Online at stacks.iop.org/JPhysCM/22/284101

Abstract
We demonstrate some recent progress in understanding the anomalous behavior of liquid water, by combining information provided by recent experiments and simulations on water in bulk, nanoconfined, and biological environments. We interpret evidence from recent experiments designed to test the hypothesis that liquid water may display 'polymorphism' in that it can exist in two different phases—and discuss recent work on water's transport anomalies as well as the unusual behavior of water in biological environments. Finally, we will discuss how the general concept of liquid polymorphism may prove useful in understanding anomalies in other liquids, such as silicon, silica, and carbon, as well as metallic glasses which have in common that they are characterized by two characteristic length scales in their interactions.

(Some figures in this article are in colour only in the electronic version)

1. Introduction

Water is perhaps the most complex liquid. Not surprisingly, then, water's phase diagram is rich and complex, with more than sixteen crystalline phases [1], and two or more glasses [2–4]. The liquid state also displays complex behavior, such as the density maximum for 1 atm at 4 °C. The volume fluctuations $\langle(\delta V)^2\rangle$, entropy fluctuations $\langle(\delta S)^2\rangle$, and cross-fluctuations between volume and entropy $\langle\delta V\delta S\rangle$, proportional to the magnitude of isothermal compressibility K_T, isobaric specific heat C_P, and isobaric thermal expansivity α_P, respectively, show anomalous increases in magnitude upon cooling [5]. Further, data on all three quantities are consistent with divergence for 1 atm at −45 °C [5], hinting at interesting phase behavior in the deeply supercooled region.

Microscopically, liquid water's anomalous behavior is understood as resulting from the tendency of neighboring molecules to form hydrogen bonds (H bonds) upon cooling, with a decrease of local potential energy, decrease of local entropy, and increase of local volume due to the formation of 'open' local structures of bonded molecules. Different models include these H bond features, but depending on the assumptions and approximations of each model, different conclusions are obtained for the low-T phase behavior. The relevant region of the liquid state cannot readily be probed experimentally, so a great deal of ingenuity has been used to obtain the results we have.

2. Four scenarios for supercooled water

Due to the difficulty of obtaining experimental evidence, theoretical and numerical analyses are useful. Four different scenarios for the pressure–temperature (P–T) phase diagram have been proposed.

(I) The *stability limit* (SL) scenario [6] hypothesizes that the superheated liquid–gas spinodal at negative pressure re-enters the positive P region below $T_H(P)$. In this view, the liquid state is delimited by a single continuous locus, $P_s(T)$, bounding the superheated, stretched and supercooled states. There is no reference to the phase into which the

liquid transforms when $P \rightarrow P_s(T)$. As the spinodal is approached, K_T, C_P, and $\alpha_P \rightarrow \infty$. A thermodynamic consequence of the SL scenario is that the intersection of the retracing spinodal with the liquid–vapor coexistence line must be a critical point [2]. The presence of such a critical point in the liquid–vapor transition, although possible, is not confirmed by any experiment. This fact poses a serious challenge to the SL scenario.

(II) The *liquid–liquid critical point* (LLCP) scenario [7] hypothesizes a first-order phase transition line between two liquids—a low density liquid (LDL), and a high density liquid (HDL)—which terminates at a liquid–liquid critical point C'. HDL is a dense liquid with a highly disordered structure, whereas LDL has a lower density and locally tetrahedral order. The experimentally observable high density amorphous (HDA) and low density amorphous (LDA) solids correspond, in this scenario, to a structurally arrested state of HDL and LDL respectively [8, 9]. Starting from C', the locus of maxima of the correlation length ξ (the Widom line) projects into the one-phase region [10]. Asymptotically close to the critical point, response functions can be expressed in terms of ξ, hence, these too will show maxima, e.g., as a function of T upon isobaric cooling. These maxima will diverge upon approaching C'. Furthermore, for $P > P_{C'}$, the pressure of C', the response functions will diverge by approaching the spinodal converging to C'. Specific models suggest [11, 7] that $P_{C'} > 0$, but the possibility $P_{C'} < 0$ has also been proposed [12, 13].

(III) The *singularity-free* (SF) scenario [14] hypothesizes that the low-T anticorrelation between volume and entropy is sufficient to cause the response functions to increase upon cooling and display maxima at non-zero T, without reference to any singular behavior [15, 16]. Specifically, Sastry *et al* [14] consider the temperature of the maximum density (TMD) line, where the density has a maximum as a function of temperature, and prove a general thermodynamic theorem establishing the proportionality between the slope of the TMD, $(\partial P/\partial T)_{\mathrm{TMD}}$, and the temperature derivative of K_T. Thus, since the TMD has negative slope in water, i.e. $(\partial P/\partial T)_{\mathrm{TMD}} < 0$, it follows that K_T must increase upon cooling, whether there exists a singularity or not.

(IV) The *critical point free* (CPF) scenario [17] hypothesizes an order–disorder transition, with possibly a weakly first-order transition character, separating two liquid phases and extending to $P < 0$ down to the superheated limit of stability of liquid water. This scenario effectively predicts a continuous locus of stability limit spanning the superheated, stretched and supercooled state, because the spinodal associated with the first-order transition will intersect the liquid–gas spinodal at negative pressure. No critical point is present in this scenario.

These four scenarios predict fundamentally different behavior, though each has been rationalized as a consequence of the same microscopic interaction: the H bond [18]. A question that naturally arises is whether the macroscopic thermodynamic descriptions are in fact connected in some way. Previous works have attempted to uncover relations between several of the scenarios, for example between (I) and (II) [11, 19] or (II) and (III) [20, 21]. Recently, Stokely *et al* [22] offered a relation linking all four scenarios showing that (a) all four can be included in one general scheme, and (b) the balance between the energies of two components of the H bond interaction determines which scenario is valid (figure 1). Moreover, they argue that current values for these energies support the LLCP scenario.

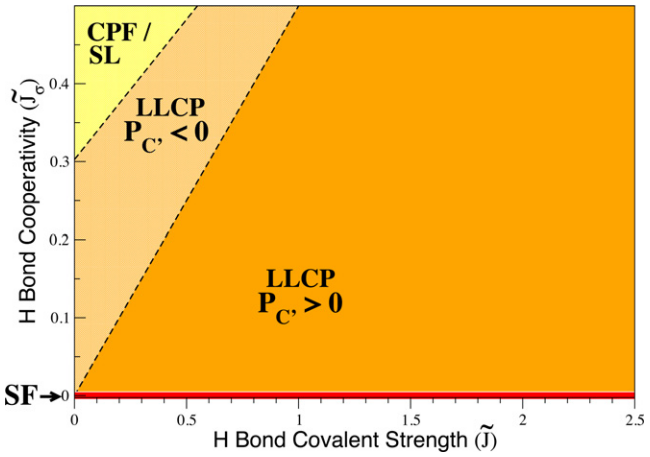

Figure 1. Possible scenarios for water for different values of H bond energies $\tilde{J}$ of the covalent (or directional) component, and $\tilde{J}_\sigma$ of the cooperative (or three-body) component, obtained from MF calculations [22]. (i) If $\tilde{J}_\sigma = 0$ (red line along x-axis), the singularity-free (SF) scenario is realized, independent of $\tilde{J}$. (ii) For large enough $\tilde{J}_\sigma$, water would possess a first-order phase transition line terminating at the liquid–gas spinodal—the critical point free (CPF) scenario; the liquid spinodal would retrace at negative pressure, as in the stability limit (SL) scenario (yellow region in top left). (iii) For other combinations of $\tilde{J}$ and $\tilde{J}_\sigma$, water would be described by the critical point (LLCP) scenario. For larger $\tilde{J}_\sigma$, the LLCP is at negative pressure (ocher region between dashed lines). For smaller $\tilde{J}_\sigma$, the LLCP is at positive pressure (orange region in bottom right). Dashed lines separating the three different regions correspond to MF results of the microscopic cell model. The P–T phase diagram evolves continuously as $\tilde{J}$ and $\tilde{J}_\sigma$ change. Courtesy of K Stokely and M Mazza.

3. Experiments

Current experiments on this problem are of two sorts. The first is a set of experiments on *bulk* water inspired by Mishima that involves probing the No Man's Land by studying the metastable extensions of the melting lines of the various high pressure polymorphs of ice: ice III, ice V, ice IV, and ice XII [23, 24]. Two of these lines clearly display 'kinks'. Since the slope of any melting line is the difference of the volume change divided by the entropy change of the two phases that coexist at that line, if there is a change in slope there must be a change in these quantities. Since there is no change in the crystal part, there must be a change in the liquid part. This means the liquid must undergo a jump in either its volume or its entropy or both. That is the definition of a first-order phase transition.

A second set of experiments is being carried out on *confined* water in the MIT group of Chen and the Messina group of Mallamace, which have stimulated many of our

recent calculations. Mallamace, Chen, and their collaborators succeeded in locating the Widom line by finding a clearcut maximum in the coefficient of thermal expansion, at $T_W \approx 225$ K [25], which remarkably is the same temperature as the specific heat maximum [49]. Also, private discussions with Klein reveal a possible reason why confined water does not freeze at $-38\,^{\circ}$C, the bulk homogeneous nucleation temperature: Klein *et al* [26] noted that confined water behaves differently from typical liquids in that water does not experience the huge increase in viscosity characteristic of other strongly confined liquids. They interpret this experimental finding as arising from the fact that strong confinement hampers the formation of a hydrogen bonded network, and we know from the classic work of Linus Pauling that without the extensive hydrogen bonded network, water's freezing temperature will be depressed by more than $100\,^{\circ}$. Thus confinement reduces the extent of the hydrogen bonded network and hence lowers the freezing temperature, but appears to leave the key tetrahedral local geometry unchanged.

Recently Gallo *et al* [27], building on their wealth of experience studying confined liquids [28–38] have accurately tested the degree to which the experiments on MCM-41 confined water are in agreement with simulations in confined geometries.

4. Experimental method of testing the singularity-free scenario

Using Monte Carlo simulations and mean field calculations, a cell model of water proposed by Franzese *et al* [39–42] can reproduce all four scenarios that have been discussed for water. Kumar *et al* [43, 44] found that both the LL critical point and singularity-free (SF) scenarios exhibit a dynamic crossover at a temperature close to $T(C_P^{\max})$, which decreases for increasing P. They interpret the dynamic crossover as a consequence of a local breaking and reorientation of the bonds for the formation of new and more tetrahedrally oriented bonds. Above $T(C_P^{\max})$, when T decreases, the number of hydrogen bonds increases, giving rise to an increasing activation energy E_A and to a non-Arrhenius dynamics. As T decreases, entropy must decrease. A major contributor to entropy is the orientational disorder, that is a function of p_B, the probability of forming a hydrogen bond, as described by the mean field expression for the entropy change ΔS with orientation. They found that, as T decreases, p_B increases. They found that the rate of increase has a maximum at $T(C_P^{\max})$, and as T continues to decrease this rate drops rapidly to zero—meaning that for $T < T(C_P^{\max})$, the local order rapidly becomes temperature-independent and the activation energy E_A also becomes approximately temperature-independent. Corresponding to this fact the dynamics becomes approximately Arrhenius.

They found that the relaxation time at the crossover temperature T_A is approximately independent of the pressure, (isochronic crossover) consistent with their calculations of an almost constant number of bonds at $T(C_P^{\max})$. They found also that in both scenarios, E_A and T_A decrease upon increasing P. Instead, the P dependence of the quantity $E_A/(k_B T_A)$ has a different behavior in the two scenarios. For the LL critical point scenario it increases as $P \to P_{C'}$, while it is approximately constant in the SF scenario. They interpret this difference as a consequence of the larger increase of the rate of change of p_B in the LL critical point scenario, where p_B diverges at finite $T_{C'}$, compared to the SF scenario, where p_B can possibly diverge only at $T = 0$. Experiments can detect local changes of water structure from HDL-like to LDL-like, (e.g., [45]). Hence, it is possible to test the predictions on the dynamic consequences of this local change. Franzese *et al* [46] found that three of the four predictions made by Kumar *et al* in [43, 44] are verified in experiments. Indeed, Chen and collaborators verified that the crossover is isochronic, and that E_A and T_A decrease upon increasing P. The fourth prediction about the behavior of $E_A/(k_B T_A)$, discriminating between the two possible scenarios, cannot be verified within the precision of the experiment [47].

5. The Widom line

By definition, in a first-order phase transitions, thermodynamic state functions such as density ρ and enthalpy H discontinuously change as we cool the system along a path crossing the equilibrium coexistence line (figure 2(a), path β). In a real experiment, this discontinuous change may not occur at the coexistence line since a substance can remain in a supercooled metastable phase until a limit of stability (a spinodal) is reached [48] (figure 2(b), path β). If the system is cooled isobarically along a path above the liquid–gas critical pressure P_c (figure 2(b), path α), the state functions continuously change from the values characteristic of a high temperature phase (gas) to those characteristic of a low temperature phase (liquid). The thermodynamic response functions, which are the derivatives of the state functions with respect to temperature (e.g., isobaric heat capacity $C_P \equiv (\partial H/\partial T)_P$) have maxima at temperatures denoted by $T_{\max}(P)$. Remarkably these maxima are still prominent far above the critical pressure [49–51], and the values of the response functions at $T_{\max}(P)$ (e.g., $C_P^{\max}$) diverge as the critical point is approached. The lines of the maxima for different response functions asymptotically approach one another as the critical point is approached, since all response functions become expressible in terms of the correlation length. This asymptotic line is sometimes called the Widom line, and is often regarded as an extension of the coexistence line into the 'one-phase regime'.

Water's anomalies have been hypothesized to be related to the existence of a line of a first-order liquid–liquid phase transition terminating at a liquid–liquid critical point [7, 23, 48, 52, 2], located below the homogeneous nucleation line in the deep supercooled region of the phase diagram—called 'no man's land' because it is difficult to make direct measurements on the *bulk* liquid phase [23]. In supercooled water, the liquid–liquid coexistence line and the Widom line have negative slopes. Thus, if the system is cooled at constant pressure P_0, computer simulations suggest that for $P_0 < P_c$ (figure 2(c), path α) experimentally measured quantities will change dramatically but continuously in the vicinity of the Widom line (with huge fluctuations as measured by, e.g., C_P) from those resembling the high density liquid

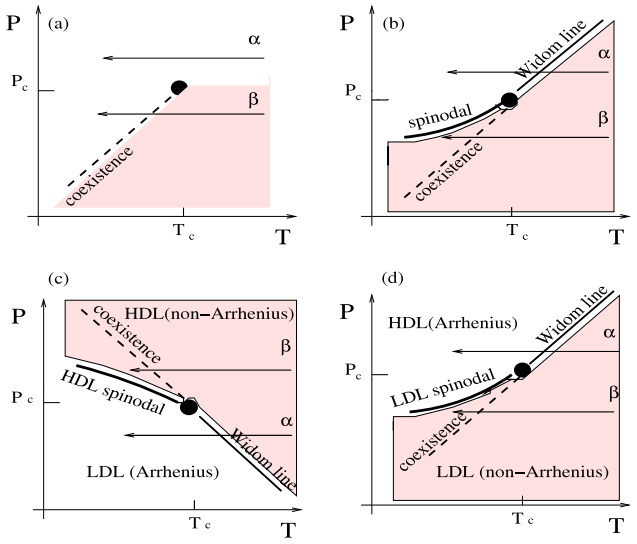

Figure 2. (a) Schematic phase diagram for the critical region associated with a liquid–gas critical point. Shown are the two features displaying mathematical singularities, the critical point (closed circles) and the liquid–gas coexistence (bold dashed curve). (b) Same as (a) with the addition of the gas–liquid spinodal and the Widom line. Along the Widom line, thermodynamic response functions have extrema in their T dependence. The path α denotes a path along which the Widom line is crossed. Path β denotes a path meeting the coexistence line. (c) A hypothetical phase diagram for water of possible relevance to the recent neutron scattering experiments by Chen *et al* [62, 63] on confined water. The liquid–liquid coexistence, which has a negative sloped coexistence line, generates a Widom line which extends below the critical point, suggesting that water may exhibit a dynamic crossover (non-Arrhenius to Arrhenius) transition for $P < P_c$ (path α), while no dynamic changes will occur above the critical point (path β). (d) A sketch of the P–T phase diagram for the two-scale Jagla model. For the Jagla potential, as well as for the double-step potential [93], the liquid–liquid phase transition line has a positive slope. Upon cooling at constant pressure above the critical point (path α), the liquid changes from a low density state (characterized by a non-glassy Arrhenius dynamics) to a high density state (characterized by glassy Arrhenius dynamics with much larger activation energy) as the path crosses the Widom line. Upon cooling at constant pressure below the critical point (path β), the liquid remains in the LDL phase as long as path β does not cross the LDL spinodal line. Thus one does not expect any change in the dynamic behavior along the path β, except upon approaching the glass transition where one can expect the non-Arrhenius behavior characterized by the Vogel–Fulcher–Tamman (VFT) fit.

HDL to those resembling the low density liquid (LDL). For $P_0 > P_c$ (figure 2(d), path β), experimentally measured quantities will change discontinuously if the coexistence line is actually seen. However, the coexistence line can be difficult to detect in a pure system due to metastability, and changes will occur only when the spinodal is approached where the HDL phase is no longer stable. The changes in behavior may include not only static quantities such as response functions [49–51] but also dynamic quantities such as diffusivity.

In the case of water, a significant change in dynamical properties has been suggested to take place in deeply supercooled states [53, 2, 54]. Unlike other network forming materials, water behaves as a non-Arrhenius liquid in the experimentally accessible window [2]. Based on analogies with other network forming liquids and with the thermodynamic properties of the amorphous forms of water, it has been suggested that, at ambient pressure, liquid water should show a dynamic crossover from non-Arrhenius behavior at high T to Arrhenius behavior at low T [55]. Using Adam–Gibbs theory [56], the dynamic crossover in water was related to the $C_P^{\max}$ line [53, 57]. Also, a dynamic crossover has been associated with the liquid–liquid phase transition in simulations of silicon and silica [58–61]. Recently a dynamic crossover in *confined* water was studied experimentally [62–64] since nucleation can be avoided in confined geometries. In this work, we interpret recent experiments on water [62–64] as arising from the presence of the hypothesized liquid–liquid critical point, which gives rise to a Widom line and an associated fragility transition (figure 2(c), path α).

6. Appearance of a fractional Stokes–Einstein relation in water and a structural interpretation of its onset

The Stokes–Einstein relation has long been regarded as one of the hallmarks of transport in liquids. It predicts that the self-diffusion constant D is proportional to $(\tau/T)^{-1}$, where τ is the structural relaxation time and T the temperature. Xu *et al* [65] recently presented experimental data on water demonstrating that, below a crossover temperature $T_\times \approx 290$ K, the Stokes–Einstein relation is replaced by a 'fractional' Stokes–Einstein relation $D \sim (\tau/T)^{-\zeta}$ with $\zeta \approx 3/5$. They interpreted the microscopic origin of this crossover by analyzing the OH stretch region of the FTIR spectrum over a wide T range from 350 down to 200 K. Simultaneous with the onset of fractional Stokes–Einstein behavior, they found that water begins to develop a local structure like that of low density amorphous solid H_2O. These data lead to an interpretation that the fractional Stokes–Einstein relation in water arises from a specific change in local water structure. To further test this interpretation, they performed computer simulations of two molecular models, and their simulation results supported their experimental observations.

They presented their experimental results on water confined in MCM-41-S nanotubes. They measured the self-diffusion D by nuclear magnetic resonance (NMR), and they measured the translational relaxation time τ by using incoherent, quasi-elastic neutron scattering (QENS) [25, 66]. Thus, the Stokes–Einstein (SE) relation,

$$D \sim (\tau/T)^{-1}, \tag{1}$$

can be tested. Their data (figure 3(a)) confirmed equation (1) at high temperatures, but showed that, upon cooling below a crossover temperature $T_\times \approx 290$ K, the SE relation (1) gave way to a 'fractional SE relation' [66–70],

$$D \sim (\tau/T)^{-\zeta}, \tag{2}$$

with $\zeta \approx 0.62$.

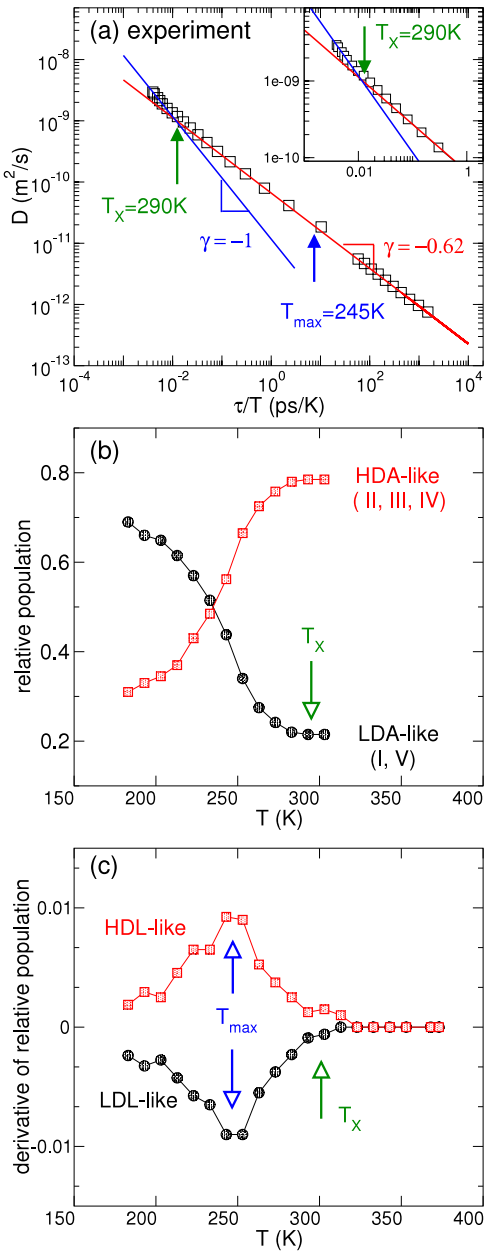

Figure 3. Experimental results for water at $P = 1$ bar. (a) Parametric relation of D as a function of τ/T. The onset of the fractional SE relation around $T_\times \approx 290$ K is indicated by the change of slope from $\zeta = 1$ to 0.62, while $T_{\max} \approx 245$ K is determined from panel (c). (b) The relative population of different species of water molecules in experiment. (i) LDA: all molecules represented by group I of the IR spectra (see section 4); (ii) HDA: all the other molecules. (c) The derivative of the relative population with respect to temperature for LDA-like and HDA-like species. Courtesy of L Xu.

As a first step to obtain a structural interpretation of this fractional SE behavior, we turn to measurements of the infrared spectrum [25, 71–73, 66]. For water this spectrum can be split into two contributions, one resembling the spectrum of high density amorphous (HDA) solid H_2O and the other resembling the spectrum of low density amorphous (LDA) solid H_2O. We interpret these two contributions as corresponding to water molecules with more HDA-like local structure, or more LDA-like local structure, respectively [74]. We show in figure 3(b) the relative populations of molecules with locally LDA-like structure and molecules with locally HDA-like structure calculated by decomposition of the infrared spectra. With decreasing T, the LDA-like population increases, while the HDA-like population decreases. The fractional SE crossover temperature $T_\times$ appears to roughly coincide with the onset of the increase of the population of molecules with LDA-like local structure (and a corresponding decrease of the population of the molecules with HDA-like local structure), consistent with the possibility that the changes in intramolecular vibrational properties may be connected to the onset of fractional SE behavior.

To more clearly see the change in the relative populations of molecules with LDA-like local structure (and, correspondingly, with HDA-like local structure), we calculate the derivatives of the relative populations with respect to temperature (figure 3(c)). The derivatives of the relative populations become noticeably non-zero at the same value of the crossover temperature, $T_\times \approx 290$ K. In contrast, we find that the maximal rate of change of the vibrational spectrum occurs at a much lower temperature, $T_{\max} \approx 245$ K, approaching the Widom temperature 225 K for bulk water [53].

Since these experiments examine water confined to cylindrical pores of ≈2 nm diameter, it is natural to question whether the findings might be instructive for understanding bulk water at low T. There are two reasons to believe that the answer is yes: (i) computer simulations of confined water on a hydrophilic surface [75] show that hydrophilic silica-confined water has similar behavior as bulk water, indicating that the hydrophilic surfaces do not have serious effects on the properties of water, except for significantly lowering the freezing temperature and stabilizing the liquid phase, which allows the study of supercooled region made impossible in bulk water due to crystallization; (ii) the presence of hysteresis in a temperature cycle (upon cooling/heating) is a signature of an interaction between water and silica. However, for the MCM-41-S confined system, only negligible hysteresis was observed by means of x-ray scattering and calorimetric experiment [76, 77]. Thus it is plausible that the MCM-41-S confined water provides information regarding bulk water.

Since experiments on bulk water at $T < 250$ K are impractical due to crystallization, we perform constant-T and constant density molecular dynamics simulations of $N = 512$ water molecules interacting with the TIP5P potential [78] at a fixed density $\rho = 1$ g cm^{-3}. Additionally, direct access to the molecular coordinates makes it possible to connect the changes in D to changes in the local molecular structure.

The relaxation time τ is defined as the time when the coherent intermediate scattering function decays by a factor of e for the wavevector q of the first peak of the static structure factor. Unlike the relaxation time of the incoherent intermediate scattering function, the coherent relaxation time closely tracks the T dependence of the viscosity (viscosity is used in the original formulation of the SE relation). The diffusion coefficient is computed from the root mean square displacement of the oxygens as a function of temperature. Analogous to the experimental results in figure 3(a), we show

the simulation results of TIP5P water for D as a function of τ/T (figure 4(a)). We see that below $T_\times \approx 320$ K the SE relation crosses over to a fractional SE relation [79] of equation (2) with $\zeta = 0.77$.

We observe in figure 4(b) a gradual increase in LDA-like local structures, and a decrease in HDA-like local structure. The derivatives of the relative populations of the LDA-like and the HDA-like molecules with respect to temperature (figure 4(c)) show that the change does not have a sharp onset at $T_\times \approx 320$ K. For each species (LDA-like and HDA-like), the maximum change defines a temperature $T_{\max} \approx 255$ K for the structural evolution [10, 80]. Like our experimental results, $T_\times > T_{\max}$ for TIP5P, indicating that the change to fractional SE behavior can be connected with the emergence of more highly structured regions of the liquid, rather than the maximal rate of change.

Both our experimental findings and our simulation results are consistent with the possibility that in water the fractional Stokes–Einstein relation (2) sets in near the temperature where the relative populations of molecules with LDA-like and HDA-like local structures start to rapidly change. A structural origin for the failure of the SE relation can be understood by recognizing that the SE relation defines an effective hydrodynamic radius. The different species have different hydrodynamic radii, so when their relative populations changes, the classical Stokes–Einstein relation (based on the assumption of the fixed hydrodynamic radius) breaks down. Moreover, a connection between the local structure of water and its dynamics is expected [81, 82, 79]; molecules with a locally tetrahedral geometry are more 'sluggish' than less well-networked molecules. This effect also occurs in solutions, where a failure of the scaling between diffusion and relaxation has been interpreted in terms of changes in the local network structure [83, 84]. For these reasons, our structure-based interpretation for the failure of the SE relation is particular to water. An explanation for the failure of the SE relation for liquids in general must involve understanding how the intermittency of the molecular motion couples to diffusion and relaxation mechanisms near the glass transition. For the majority of liquids, the breakdown of SE occurs within 30% of the glass transition temperature, while for water it occurs at almost twice the glass transition temperature. For the case of water, the emergence of such intermittency of the dynamics is inseparable from water's unusual thermodynamics and corresponding changes in the fluid structure.

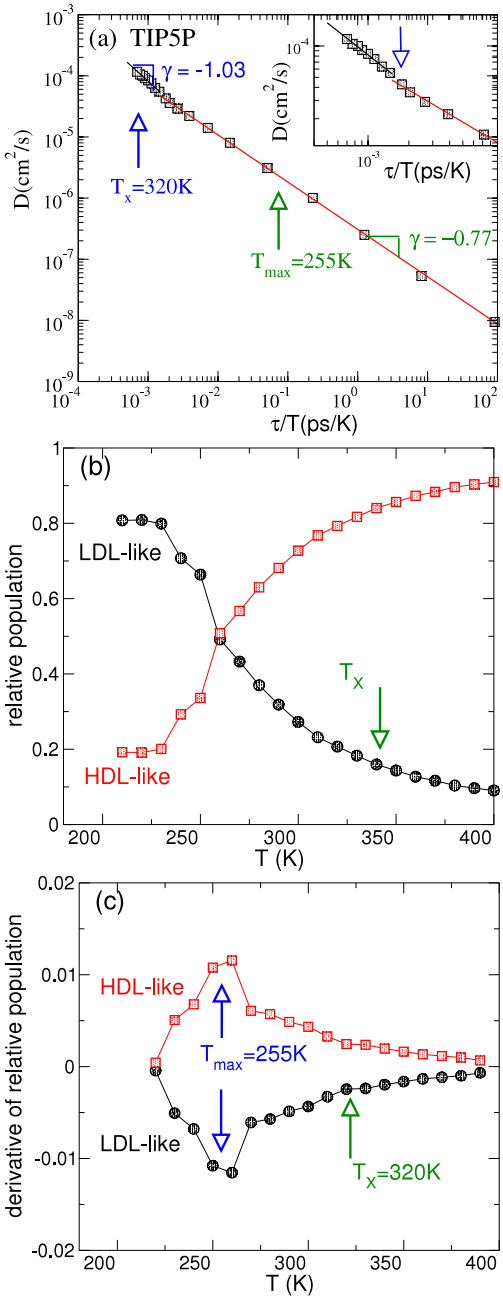

Figure 4. Analog of figure 3 for bulk TIP5P water. (a) Parametric relation of D as a function of τ/T. The SE relation breaks down around $T \approx 320$ K, while $T_{\max} \approx 255$ K. (b) The relative population of different species of molecules in simulation for TIP5P along paths of constant density $\rho = 1.00$ g cm^{-3}. Different species are defined according to the local tetrahedral order Q_i for each molecule i. We define a molecule as (i) LDA-like if $Q > 0.80$ and (ii) HDA-like if $Q \leqslant 0.8$. The crossing of relative populations of LDA and HDA corresponds to the temperature where the specific heat C_P shows a maximum, similar to the experimental results in figure 3(b). (c) Derivative of the relative population with respect to temperature. For each species (LDA and HDA), the maximum changes occurs at $T_{\max} \approx 255$ K. The breakdown of the SE relation occurs at temperature $T_\times$ when each species start to change more rapidly. Courtesy of L Xu.

7. The tetrahedral entropy and tetrahedral specific heat reflecting space–time correlations in the tetrahedral order parameter

Very recently Kumar *et al* [80] introduced the space-dependent correlation function $C_Q(r)$ and time-dependent autocorrelation function $C_Q(t)$ of the local tetrahedral order parameter $Q \equiv Q(r, t)$ [85]. Using computer simulations of 512 waterlike particles interacting through the TIP5P potential, they investigated $C_Q(r)$ in a broad region of the phase diagram. They found that at low temperatures $C_Q(t)$ exhibits a two-step time-dependent decay similar to the self-intermediate scattering function, and that the corresponding correlation time

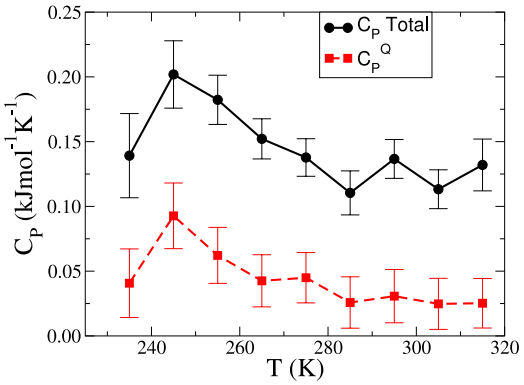

Figure 5. Constant pressure specific heat C_P and specific heat associated with the tetrahedral entropy C_P^Q of water at atmospheric pressure for the TIP5P model of water. Courtesy of P Kumar.

τ_Q displays a dynamic crossover from non-Arrhenius behavior for $T > T_W$ to Arrhenius behavior for $T < T_W$, where T_W denotes the Widom temperature where the correlation length has a maximum as T is decreased along a constant pressure path. They defined a tetrahedral entropy S_Q associated with the *local* tetrahedral order of water molecules and found that it produces a major contribution to the specific heat maximum at the Widom line (figure 5), and showed that τ_Q can be extracted from S_Q using an analog of the Adam–Gibbs relation.

8. Dynamic crossover at the Widom line

Using molecular dynamics (MD) simulations [86], Xu *et al* [10] studied three models, each of which appears to have a liquid–liquid critical point. Two of the models (the TIP5P [87] and the ST2 [88]) treat water as a multiple site rigid body, interacting via electrostatic site–site interactions complemented by a Lennard-Jones potential. The third model is the spherical 'two-scale' Jagla potential with attractive and repulsive ramps which has been studied in the context of liquid–liquid phase transitions and liquid anomalies [51, 55, 89, 90]. For all three models, Xu *et al* evaluated the loci of maxima of the relevant response functions, compressibility and specific heat, which coincide close to the critical point and give rise to the Widom line. They found evidence that, for all three potentials, the dynamic crossover occurs just when the Widom line is crossed.

Still another model has been studied, SPC/E, but the temperature shift is about 40 K since SPC/E is under-structured compared to real water as it collapses the two negatively charged lone pairs into a single negative point charge. Hence at such low temperatures the statistics are not very good for recognizing the critical point [91].

Other models, which are particularly tractable, include a family of spherically symmetric potentials pioneered by Stell and Hemmer which are characterized by two length scales and hence reflect many of the properties of real water (see, e.g., [92, 93] and references therein).

These findings are consistent with the possibility that the observed dynamic crossover along path α is related to the behavior of C_P, suggesting that enthalpy or entropy fluctuations may have a strong influence on the dynamic properties [51, 53, 61, 53]. Indeed, as the thermodynamic properties change from the high temperature side of the Widom line to the low temperature side, $(\partial S/\partial T)_P = C_P/T > 0$ implies that the entropy must decrease. The entropy decrease is most pronounced at the Widom line when $C_P = C_P^{\max}$. Since the configurational part of the entropy, $S_{\rm conf}$, makes the major contribution to S, we expect that $S_{\rm conf}$ also decreases sharply on crossing the Widom line.

According to Adam–Gibbs theory [56], $D \sim \exp(-A/TS_{\rm conf})$. Hence, we expect that D sharply decreases upon cooling at the Widom line. If $S_{\rm conf}$ does not change appreciably with T, then the Adam–Gibbs equation predicts an Arrhenius behavior of D. For both water and the Jagla model, crossing the Widom line is associated with the change in the behavior of the diffusivity. (i) In the case of water, D changes from non-Arrhenius to Arrhenius behavior, while the structural and thermodynamic properties change from those resembling HDL to those resembling LDL, due to the *negative* slope of the Widom line. (ii) For the Jagla potential, D changes from Arrhenius to non-Arrhenius while the structural and thermodynamic properties change from those resembling LDL to those resembling HDL, due to the *positive* slope of the Widom line.

Thus these results for bulk water are consistent with the experimental observation in confined water of (i) a fragility transition for $P < P_c$ [62, 63], and (ii) a peak in C_P upon cooling water at atmospheric pressure [94], so this work offers a plausible interpretation of the results of [63] as supporting the existence of a hypothesized liquid–liquid critical point.

9. Glass transition in biomolecules

Next we explore the rather novel hypothesis [95] that the observed glass transition in biomolecules [96, 78] is related to the liquid–liquid phase transition using molecular dynamics (MD) simulations. Specifically, Kumar *et al* [95] studied the dynamic and thermodynamic behavior of lysozyme and DNA in hydration TIP5P water, by means of the software package GROMACS for (i) an orthorhombic form of hen egg-white lysozyme and (ii) a Dickerson dodecamer DNA at constant pressure $P = 1$ atm, several constant temperatures T, and constant number of water molecules N (NPT ensemble).

The simulation results for the mean square fluctuations $\langle x^2\rangle$ of both protein and DNA are shown in figure 6(a). Kumar *et al* calculated the mean square fluctuations $\langle x^2\rangle$ of the biomolecules from the equilibrated configurations, first for each atom over 1 ns, and then averaged over the total number of atoms in the biomolecule. They find that $\langle x^2\rangle$ changes its functional form below $T_p \approx 245$ K, for *both* lysozyme (figure 6(a)) and DNA (figure 6(b)).

Kumar *et al* next calculated C_P by numerical differentiation of the total enthalpy of the system (protein and water) by fitting the simulation data for enthalpy with a fifth order polynomial, and then taking the derivative with respect to T. Figures 7(a) and (b) display maxima of $C_P(T)$ at $T_W \approx 250 \pm 10$ K for both biomolecules.

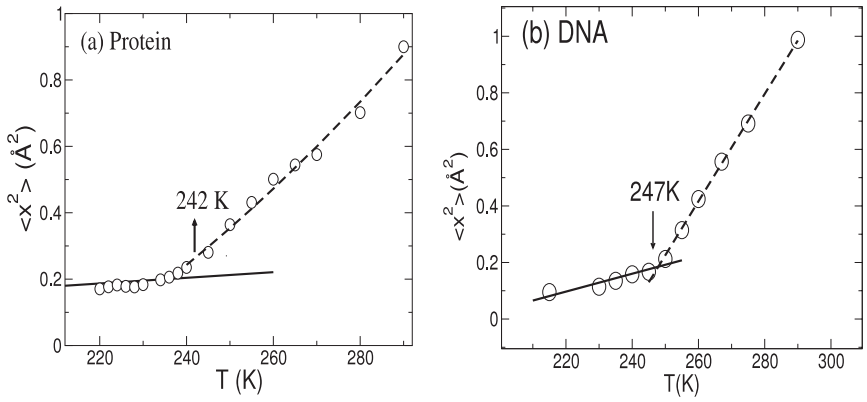

Figure 6. Mean square fluctuation of (a) lysozyme, and (b) DNA showing that there is a transition around $T_p \approx 242 \pm 10$ K for lysozyme and around $T_p \approx 247 \pm 10$ K for DNA. For very low T one would expect a linear increase of $\langle x^2 \rangle$ with T, as a consequence of the harmonic approximation for the motion of residues. At high T, the motion becomes non-harmonic and we fit the data by a polynomial. We determine the dynamic crossover temperature T_p from the crossing of the linear fit for low T and the polynomial fit for high T. We determine the error bars by changing the number of data points in the two fitting ranges. Courtesy of P Kumar.

Further, to describe the quantitative changes in structure of hydration water, Kumar *et al* calculated the local tetrahedral order parameter Q [85, 97–99] for hydration water surrounding lysozyme and DNA. Figures 7(c) and (d) show that the rate of increase of Q has a maximum at 245 ± 10 K for lysozyme and DNA hydration water respectively; the same temperatures of the crossover in the behavior of mean square fluctuations.

Upon cooling, the diffusivity of hydration water exhibits a dynamic crossover from non-Arrhenius to Arrhenius behavior at the crossover temperature $T_\times \approx 245 \pm 10$ K (figure 7(e)). The coincidence of $T_\times$ with T_p, within the error bars, indicates that the behavior of the protein is strongly coupled with the behavior of the surrounding solvent, in agreement with recent experiments [96]. Note that $T_\times$ is much higher than the glass transition temperature, estimated for TIP5P as $T_g = 215$ K [100]. Thus this crossover is not likely to be related to the glass transition in water.

The fact that $T_p \approx T_\times \approx T_W$ is evidence of the correlation between the changes in protein fluctuations (figure 6(a)) and the hydration water thermodynamics (figure 7(a)). Thus these results are consistent with the possibility that the protein glass transition is related to the Widom line (and hence to the hypothesized liquid–liquid critical point). Crossing the Widom line corresponds to a continuous but rapid transition of the properties of water from those resembling the properties of a local HDL structure for $T > T_W(P)$ to those resembling the properties of a local LDL structure for $T < T_W(P)$ [10, 63]. A consequence is the expectation that the fluctuations of the protein residues in predominantly LDL-like water (more ordered and more rigid) just below the Widom line should be smaller than the fluctuations in predominantly HDL-like water (less ordered and less rigid) just above the Widom line.

The quantitative agreement of the results for both DNA and lysozyme (figures 6 and 7) suggests that it is indeed the changes in the properties of hydration water that are responsible for the changes in dynamics of the protein and DNA biomolecules. Our results are in qualitative agreement with recent experiments on hydrated protein and DNA which found the crossover in side-chain fluctuations at $T_p \approx 225$ K.

10. Outlook

It is possible that other phenomena that appear to occur on crossing the Widom line are in fact not coincidences, but are related to the changes in local structure that occur when the system changes from the 'HDL-like' side to the 'LDL-like' side. In this work we concentrated on reviewing the evidence for changes in dynamic transport properties, such as diffusion constant and relaxation time. Additional examples include: (1) a breakdown of the Stokes–Einstein relation for $T < T_W(P)$ [80, 66, 79, 68], (2) systematic changes in the static structure factor $S(q)$ and the corresponding pair correlation function $g(r)$ revealing that for $T < T_W(P)$ the system more resembles the structure of LDL than HDL, (3) the appearance for $T < T_W(P)$ of a shoulder in the dynamic structure factor $S(q, \omega)$ at a frequency $\omega \approx 60\ \text{cm}^{-1} \approx 2$ THz [96], (4) a rapid increase in hydrogen bonding degree for $T < T_W(P)$ [43], (5) a *minimum* in the density at low temperature [101], and (6) a scaled equation of state near the critical point [102]. It is important to know how general a given phenomenon is, such as crossing the Widom line, which by definition is present whenever there is a critical point. Using data on other liquids which have local tetrahedral symmetry, such as silicon and silica, which also appear to display a liquid–liquid critical point and hence must possess a Widom line emanating from this point into the one-phase region. For example, Morishita interprets structural changes in silicon as arising from crossing the Widom line [103]. Underway are tests of the effect of the Widom line on simple model systems that display a liquid–liquid critical point, such as two-scale symmetric potentials of the sort recently studied by Xu and collaborators [51, 104]. It is becoming clear that a local tetrahedral symmetry matters because it is associated with two characteristic length scales in the interaction potential. Other systems, such as metallic glasses, also appear to be two-scale and there is evidence of polymorphism [105].

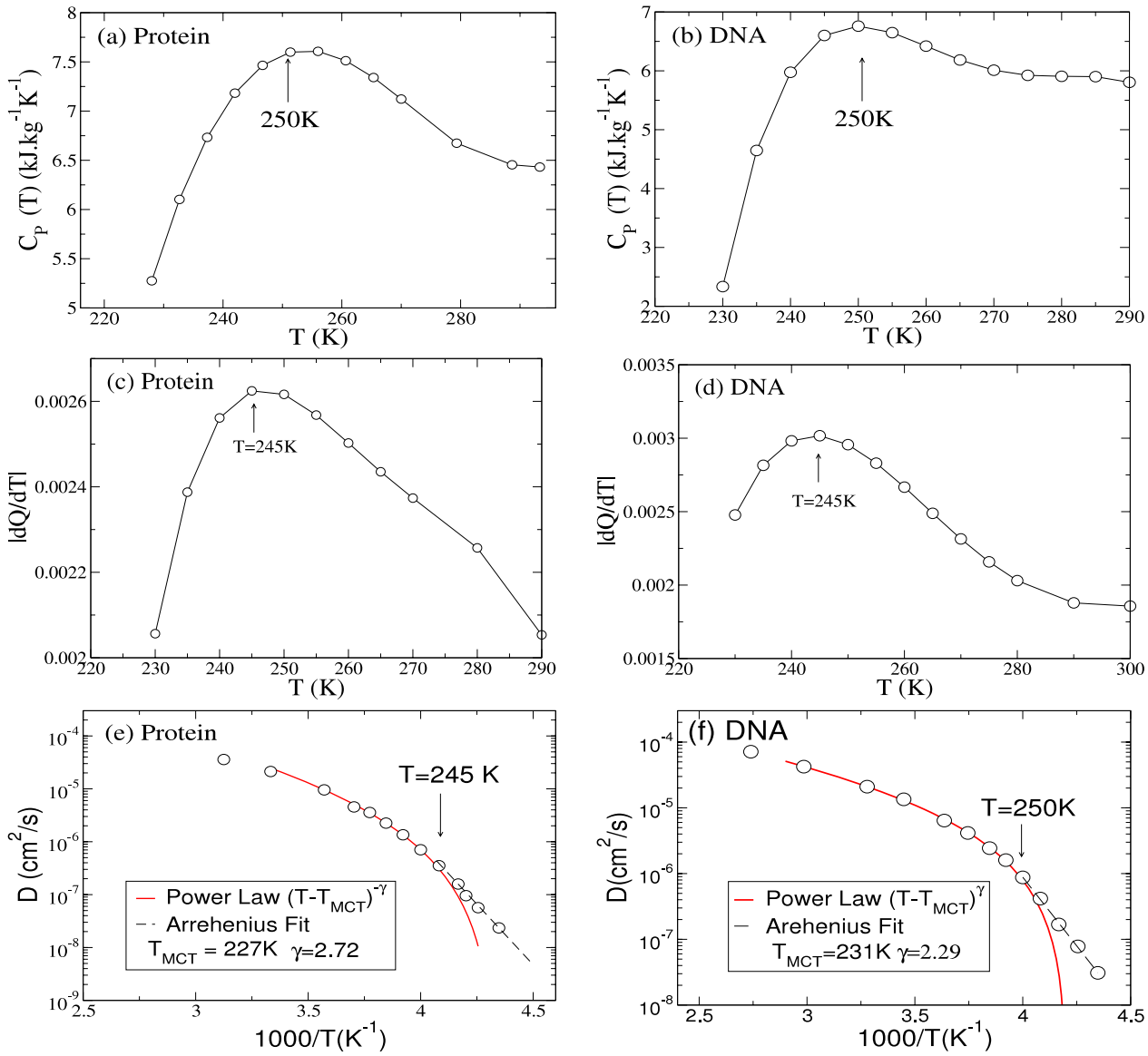

Figure 7. The specific heat of the combined system (a) lysozyme and water, and (b) DNA and water, display maxima at 250 ± 10 K and 250 ± 12 K respectively, which are coincident within the error bars with the temperature T_p where the crossover in the behavior of $\langle x^2 \rangle$ is observed in figure 2. Derivative with respect to temperature of the local tetrahedral order parameter Q for (c) lysozyme and (d) DNA hydration water. A maximum in $|dQ/dT|$ at Widom line temperature suggests that the rate of change of local tetrahedrality of hydration water has a maximum at the Widom line. The diffusion constant of hydration water surrounding (e) lysozyme, and (f) DNA shows a dynamic transition from a power law behavior to an Arrhenius behavior at $T_\times \approx 245 \pm 10$ K for lysozyme and $T_\times \approx 250 \pm 10$ K for DNA, around the same temperatures where the behavior of $\langle x^2 \rangle$ has a crossover, and C_P and $|dQ/dT|h$ have maxima. Courtesy of P Kumar.

Acknowledgments

This paper is a contribution that concerns recent progresses in the field of computer simulations of water discussed at the CECAM workshop 'Modeling and Simulation of Water at Interfaces from Ambient to Supercooled Conditions' supported by ESF-Simbioma and CECAM.

This work has been carried out with many collaborators, of whom only a small number have joined this paper as co-authors. The work has been heavily influenced by a number of excellent experimentalists, including C A Angell [11], M C Bellissent-Funel [8], L Bosio [106], F Bruni, S-H Chen [95, 107, 10], D Leporini [108], L Liu [63], F Mallamace [25, 109–112], O Mishima [113, 114, 23], A Nilsson [115], J Teixeira [15, 16] and by the very experienced computational chemist, A Geiger [116, 117]. The work at Boston University was supported by the Chemistry Division of the NSF. SVB thanks the Office of the Academic Affairs of Yeshiva University for funding the Yeshiva University high-performance computer cluster and acknowledges the partial support of this research through the Dr Bernard W Gamson Computational Science Center at Yeshiva College. GF thanks the Spanish Ministerio de Ciencia e Innovación grant FIS2009-10210 (co-financed FEDER). XLM acknowledges the support by the World Premier International Research Center Initiative (WPI Initiative), MEXT, Japan.

References

[1] Zheligovskaya E A and Malenkov G G 2006 Crystalline water ices *Russ. Chem. Rev.* **75** 57–76

[2] Debenedetti P G 2003 Supercooled and glassy water *J. Phys.: Condens. Matter* **15** R1669–726

[3] Loerting T and Giovambattista N 2006 Amorphous ices: experiments and numerical simulations *J. Phys.: Condens. Matter* **18** R919–77

[4] Kim C U, Barstow B, Tate M W and Gruner S M 2009 Evidence for liquid water during the high-density to low-density amorphous ice transition *Proc. Natl Acad. Sci. USA* **106** 4596–600

[5] Angell C A 1982 *Water: A Comprehensive Treatise* vol 7, ed F Franks (New York: Plenum) pp 1–81

[6] Speedy R J 1982 Limiting forms of the thermodynamic divergences at the conjectured stability limits in superheated and supercooled water *J. Phys. Chem.* **86** 3002–5

[7] Poole P H, Sciortino F, Essmann U and Stanley H E 1992 Phase behavior of metastable water *Nature* **360** 324–8

[8] Starr F W, Bellissent-Funel M-C and Stanley H E 1999 Continuity of liquid and glassy water *Phys. Rev.* E **60** 1084–7

[9] Bellissent-Funel M C and Bosio L 1995 A neutron scattering study of liquid D_2O *J. Chem. Phys.* **102** 3727–35

[10] Xu L, Kumar P, Buldyrev S V, Chen S-H, Poole P H, Sciortino F and Stanley H E 2005 Relation between the Widom line and the dynamic crossover in systems with a liquid–liquid critical point *Proc. Natl Acad. Sci.* **102** 16558–62

[11] Poole P H, Sciortino F, Grande T, Stanley H E and Angell C A 1994 Effect of hydrogen bonds on the thermodynamic behavior of liquid water *Phys. Rev. Lett.* **73** 1632–5

[12] Tanaka H 1996 A self-consistent phase diagram for supercooled water *Nature* **380** 328–30

[13] Tanaka H 1996 Phase behaviors of supercooled water: reconciling a critical point of amorphous ices with spinodal instability *J. Chem. Phys.* **105** 5099–111

[14] Sastry S, Debenedetti P, Sciortino F and Stanley H E 1996 Singularity-free interpretation of the thermodynamics of supercooled water *Phys. Rev.* E **53** 6144–54

[15] Stanley H E 1979 A polychromatic correlated-site percolation problem with possible relevance to the unusual behavior of supercooled H_2O and D_2O *J. Phys. A: Math. Gen.* **12** L329–37

[16] Stanley H E and Teixeira J 1980 Interpretation of the unusual behavior of H_2O and D_2O at low temperatures: tests of a percolation model *J. Chem. Phys.* **73** 3404–22

[17] Angell C A 2008 Insights into phases of liquid water from study of its unusual glass-forming properties *Science* **319** 582–7

[18] Starr F W, Nielsen J K and Stanley H E 1999 Fast and slow dynamics of hydrogen bonds in liquid water *Phys. Rev. Lett.* **82** 2294–7

[19] Borick S S, Debenedetti P G and Sastry S 1995 A lattice model of network-forming fluids with orientation-dependent bonding: equilibrium, stability, and implications from the phase behavior of supercooled water *J. Phys. Chem.* **99** 3781–93

[20] Truskett T M, Debenedetti P G, Sastry S and Torquato S 1999 A single-bond approach to orientation-dependent interactions and its implications for liquid water *J. Chem. Phys.* **111** 2647–56

[21] Tanaka H 2000 Thermodynamic anomaly and polyamorphism of water *Europhys. Lett.* **50** 340–6

[22] Stokely K, Mazza M G, Stanley H E and Franzese G 2010 Effect of hydrogen bond cooperativity on the behavior of water *Proc. Natl Acad. Sci. USA* **107** 1301–6

[23] Mishima O and Stanley H E 1998 Decompression-induced melting of Ice IV and the liquid–liquid transition in water *Nature* **392** 164–8

[24] Mishima O 2000 Liquid–liquid critical point in heavy water *Phys. Rev. Lett.* **85** 334–6

[25] Mallamace F, Broccio M, Corsaro C, Faraone A, Majolino D, Venuti V, Liu L, Mou C Y and Chen S-H 2007 Evidence of the existence of the low-density liquid phase in supercooled, confined water *Proc. Natl Acad. Sci. USA* **104** 424–8

[26] Raviv U, Laurat P and Klein J 2001 Fluidity of water confined to subnanometre films *Nature* **413** 51–4

[27] Gallo P, Rovere M and Chen S-H 2010 Dynamic crossover in supercooled confined water: understanding bulk properties through confinement *J. Phys. Chem. Lett.* **1** 729–33

[28] Gallo P, Attili A and Rovere M 2009 Mode-coupling behavior of a Lennard-Jones binary mixture upon increasing confinement *Phys. Rev.* E **80** 061502

[29] De Grandis V, Gallo P and Rovere M 2007 The phase diagram of confined fluids *European/Japanese Molecular Liquids Groups Interdisciplinary Conf. (Prague, Sept. 2005)*; *J. Mol. Liq.* **134** 90–3

[30] De Grandis V, Gallo P and Rovere M 2006 Liquid–liquid coexistence in the phase diagram of a fluid confined in fractal porous materials, *Europhys. Lett.* **75** 901–7

[31] Attili A, Gallo P and Rovere M 2005 Mode coupling behavior of a Lennard-Jones binary mixture: a comparison between bulk and confined phases *J. Chem. Phys.* **123** 174510

[32] Gallo P, Attili A and Rovere M 2004 Slow dynamics of a confined supercooled binary mixture in comparison with the bulk phase *9th Int. Workshop on Disordered Systems (Molveno Andalo, March 2003)*; *Phil. Mag.* **84** 1397–404

[33] Gallo P, Pellarin R and Rovere M 2003 Slow dynamics of a confined supercooled binary mixture: II. Q space analysis *Phys. Rev.* E **68** 061209

[34] Gallo P and Rovere M 2003 Anomalous dynamics of confined water at low hydration *J. Phys.: Condens. Matter* **15** 7625–33

[35] Gallo P, Rovere M and Spohr E 2000 Supercooled confined water and the mode coupling crossover temperature *Phys. Rev. Lett.* **85** 4317–20

[36] Attili A, Gallo P and Rovere M 2005 Inherent structures and Kauzmann temperature of confined liquids *Phys. Rev.* E **71** 031204

[37] Gallo P and Rovere M 2003 Double dynamical regime of confined water *J. Phys.: Condens. Matter* **15** 1521–9

[38] Rovere M and Gallo P 2003 Effects of confinement on static and dynamical properties of water *Eur. Phys. J.* E **12** 77–81

[39] Franzese G and Stanley H E 2002 Liquid–liquid critical point in a Hamiltonian model for water: analytic solution *J. Phys.: Condens. Matter* **14** 2201–9

[40] Franzese G and Stanley H E 2002 A theory for discriminating the mechanism responsible for the water density anomaly *Physica* A **314** 508

[41] Franzese G and Stanley H E 2007 The Widom line of supercooled water *J. Phys.: Condens. Matter* **19** 205126

[42] Franzese G, Marqu'es M I and Stanley H E 2003 Intramolecular coupling as a mechanism for a liquid–liquid phase transition *Phys. Rev.* E **67** 011103

[43] Kumar P, Franzese G and Stanley H E 2008 Predictions of dynamic behavior under pressure for two scenarios to explain water anomalies *Phys. Rev. Lett.* **100** 105701

[44] Kumar P, Franzese G and Stanley H E 2008 Dynamics and thermodynamics of water *J. Phys.: Condens. Matter* **20** 244114

[45] Li F-F, Cui Q-L, He Z, Zhang J, Zhou Q and Zou G-T 2005 High pressure-temperature Brillouin study of liquid water: evidence of the structural transition from low-density water to high-density water *J. Chem. Phys.* **123** 174511

[46] Franzese G, Stokely K, Chu X-Q, Kumar P, Mazza M G, Chen S-H and Stanley H E 2008 Pressure effects in supercooled water: comparison between a 2D model of water and experiments for surface water on a protein *J. Phys.: Condens. Matter* **20** 494210

[47] Chu X-Q, Faraone A, Kim C, Fratini E, Baglioni P, Leao J B and Chen S-H 2009 Proteins remain soft at lower temperatures under pressure *J. Phys. Chem.* B **113** 5001–6

[48] Debenedetti P G and Stanley H E 2003 The physics of supercooled and glassy water *Phys. Today* **56** (6) 40–6

[49] Anisimov M A, Sengers J V and Levelt Sengers J M H 2004 Near-critical behavior of aqueous systems *Aqueous System at Elevated Temperatures and Pressures: Physical Chemistry in Water, Stream and Hydrothermal Solutions* ed D A Palmer, R Fernandez-Prini and A H Harvey (Amsterdam: Elsevier)

[50] Levelt J M H 1958 Measurements of the compressibility of argon in the gaseous and liquid phase *PhD Thesis* University of Amsterdam, Van Gorkum

[51] Xu L, Buldyrev S V, Angell C A and Stanley H E 2006 Thermodynamics and Dynamics of the Two-Scale Spherically Symmetric Jagla ramp model of anomalous liquids *Phys. Rev.* E **74** 031108

[52] Mallamace F 2009 The liquid water polymorphism *Proc. Natl Acad. Sci. USA* **106** 15097–8

[53] Starr F W, Angell C A and Stanley H E 2003 Prediction of entropy and dynamic properties of water below the homogeneous nucleation temperature *Physica* A **323** 51–66

[54] Kumar P, Buldyrev S V, Starr F, Giovambattista N and Stanley H E 2005 Thermodynamics, structure, and dynamics of water confined between hydrophobic plates *Phys. Rev.* E **72** 051503

[55] Jagla E A 1999 Core-softened potentials and the anomalous properties of water *J. Chem. Phys.* **111** 8980–6

[56] Adam G and Gibbs J H 1965 On the temperature dependence of cooperative relaxation properties in glass-forming liquids *J. Chem. Phys.* **43** 139–46

[57] Poole P H, Saika-Voivod I and Sciortino F 2005 Density minimum and liquid–liquid phase transition *J. Phys.: Condens. Matter* **17** L431–7

[58] Sastry S and Angell C A 2003 Liquid–liquid phase transition in supercooled silicon *Nat. Mater.* **2** 739–43

[59] Ganesh P and Widom M 2009 Liquid–liquid transition in supercooled silicon determined by first-principles simulation *Phys. Rev. Lett.* **102** 075701

[60] Beye M, Sorgenfrei F, Schlotter W F, Wurth W and Frhlisch A 2010 The liquid–liquid phase transition in silicon revealed by snapshots of valence electrons, at press

[61] Saika-Voivod I, Poole P H and Sciortino F 2001 Fragile-to-strong transition and polyamorphism in the energy landscape of liquid silica *Nature* **412** 514–7

[62] Faraone A, Liu L, Mou C-Y, Yen C-W and Chen S-H 2004 Fragile-to-strong liquid transition in deeply supercooled confined water *J. Chem. Phys.* **121** 10843–6

[63] Liu L, Chen S-H, Faraone A, Yen C-W and Mou C Y 2005 Pressure dependence of fragile-to-strong transition and a possible second critical point in supercooled confined water *Phys. Rev. Lett.* **95** 117802

[64] Mallamace F, Broccio M, Corsaro C, Faraone A, Wanderlingh U, Liu L, Mou C Y and Chen S-H 2006 The fragile-to-strong dynamic crossover transition in confined water: nuclear magnetic resonance results *J. Chem. Phys.* **124** 161102

[65] Xu L, Mallamace F, Yan Z, Starr F W, Buldyrev S V and Stanley H E 2009 appearance of a fractional Stokes–Einstein relation in water and a structural interpretation of its onset *Nat. Phys.* **5** 565–9

[66] Chen S-H, Mallamace F, Mou C-Y, Broccio M, Corsaro C, Faraone A and Liu L 2006 The violation of the Stokes–Einstein relation in supercooled water *Proc. Natl Acad. Sci. USA* **103** 12974–8

[67] Becker S R, Poole P H and Starr F W 2006 Fractional Stokes–Einstein and Debye–Stokes–Einstein relations in a network-forming liquid *Phys. Rev. Lett.* **97** 055901

[68] Mazza M G, Giovambattista N, Stanley H E and Starr F W 2007 Breakdown of the Stokes–Einstein and Stokes–Einstein–Debye relations and dynamics heterogeneities in a molecular system *Phys. Rev.* E **76** 031203

[69] Fernandez-Alonson F, Bermejo F J, McLain S E, Turner J F C, Molaison J J and Herwig K W 2007 Observation of fractional Stokes–Einstein behavior in the simplest hydrogen-bonded liquid *Phys. Rev. Lett.* **98** 077801

[70] Douglas J F and Leporini D 1998 Obstruction model of the fractional Stokes–Einstein relation in glass-forming liquids *J. Non-Cryst. Solids* **235** 137–41

[71] Soper A K and Ricci M A 2000 Structures of high-density and low-density water *Phys. Rev. Lett.* **84** 2881–4

[72] Zanotti J M, Bellissent-Funel M C and Chen S-H 2005 Experimental evidence of a liquid–liquid transition in interfacial water *Europhys. Lett.* **71** 91–7

[73] Walrafen G E, Hokmababi M S and Yang W H A 1986 Raman isosbestic points from liquid water *J. Chem. Phys.* **85** 6964–9

[74] Canpolat M, Starr F W, Sadr-Lahijany M R, Scala A, Mishima O, Havlin S and Stanley H E 1998 Local structural heterogeneities in liquid water under pressure *Chem. Phys. Lett.* **294** 9–12

[75] Giovambattista N, Rossky P J and Debenedetti P G 2006 Effect of pressure on the phase behavior and structure of water confined between nanoscale hydrophobic and hydrophilic plates *Phys. Rev.* E **73** 041604

[76] Morishige K and Nobuoka K 1997 X-ray diffraction studies of freezing and melting of water confined in a mesoporous adsorbent (MCM-41) *J. Chem. Phys.* **107** 6965–9

[77] Schreiber A, Schreiber A, Ketelsen I and Findenegg G H 2001 Melting and freezing of water in ordered mesoporous silica materials *Phys. Chem. Chem. Phys.* **3** 1185–95

[78] Yamada M, Mossa S, Stanley H E and Sciortino F 2002 Interplay between time-temperature-transformation and the liquid–liquid phase transition in water *Phys. Rev. Lett.* **88** 195701

[79] Mazza M G, Giovambattista N, Starr F W and Stanley H E 2006 Relation between rotational and translational dynamic heterogeneities in water *Phys. Rev. Lett.* **96** 057803

[80] Kumar P, Buldyrev S V and Stanley H E 2009 A tetrahedral entropy for water *Proc. Natl Acad. Sci. USA* **106** 22130–4

[81] Sciortino F, Poole P, Stanley H E and Havlin S 1990 Lifetime of the hydrogen bond network and gel-like anomalies in supercooled water *Phys. Rev. Lett.* **64** 1686–9

[82] Giovambattista N, Starr F W, Sciortino S, Buldyrev S V and Stanley H E 2002 Transitions between inherent structures in water *Phys. Rev.* E **65** 041502

[83] Molinero V and Moore E B 2009 Water modeled as an intermediate element between carbon and silicon *J. Phys. Chem.* B **113** 4008–16

[84] Moore E B and Molinero V 2009 Growing correlation length in supercooled water *J. Chem. Phys.* **130** 244505

[85] Errington J R and Debenedetti P G 2001 Relationship between structural order and the anomalies of liquid water *Nature* **409** 318–21

[86] Rapaport D C 1995 *The Art of Molecular Dynamics Simulation* (Cambridge: Cambridge University Press)

[87] Mahoney M W and Jorgensen W L 2000 A five-site model for liquid water and the reproduction of the density anomaly by rigid, nonpolarizable potential functions *J. Chem. Phys.* **112** 8910–22

[88] Stillinger F H and Rahman A 1972 Molecular dynamics study of temperature effects on water structure and kinetics *J. Chem. Phys.* **57** 1281–92
[89] Kumar P, Buldyrev S V, Sciortino F, Zaccarelli E and Stanley H E 2005 Static and dynamic anomalies in a repulsive spherical ramp liquid: theory and simulation *Phys. Rev.* E **72** 021501
[90] Xu L, Ehrenberg I, Buldyrev S V and Stanley H E 2006 Relationship between the liquid–liquid phase transition and dynamic behavior in the Jagla model *J. Phys.: Condens. Matter* **18** S2239–46
[91] Harrington S, Poole P H, Sciortino F and Stanley H E 1997 Equation of state of supercooled SPC/E water *J. Chem. Phys.* **107** 7443–50
[92] Sadr-Lahijany M R, Scala A, Buldyrev S V and Stanley H E 1998 Liquid state anomalies for the Stell-Hemmer core-softened potential *Phys. Rev. Lett.* **81** 4895–8
[93] Franzese G, Malescio G, Skibinsky A, Buldyrev S V and Stanley H E 2001 Generic mechanism for generating a liquid–liquid phase transition *Nature* **409** 692–5 (arXiv:cond-mat/0102029)
[94] Maruyama S, Wakabayashi K and Oguni M 2004 Thermal properties of supercooled water confined within silica gel pores *AIP Conf. Proc.* **708** 675–6
[95] Kumar P, Yan Z, Xu L, Mazza M G, Buldyrev S V, Chen S-H, Sastry S and Stanley H E 2006 Glass transition in biomolecules and the liquid–liquid critical point of water *Phys. Rev. Lett.* **97** 177802
[96] Chen S-H, Liu L, Fratini E, Baglioni P, Faraone A and Mamontov E 2006 The observation of fragile-to-strong dynamic crossover in protein hydration water *Proc. Natl Acad. Sci. USA* **103** 9012
[97] Yan Z, Buldyrev S V, Giovambattista N and Stanley H E 2005 Structural order for one-scale and two-scale potentials *Phys. Rev. Lett.* **95** 130604
[98] Yan Z, Buldyrev S V, Giovambattista N, Debenedetti P G and Stanley H E 2006 Family of tunable spherically-symmetric potentials that span the range from hard spheres to water-like behavior *Phys. Rev.* E **73** 051204
[99] Yan Z, Buldyrev S V, Kumar P, Giovambattista N, Debenedetti P G and Stanley H E 2007 Structure of the first- and second-neighbor shells of simulated water: quantitative relation to translational and orientational order *Phys. Rev.* E **76** 051201
[100] Brovchenko I, Geiger A and Oleinikova A 2005 Liquid–liquid phase transitions in supercooled water studied by computer simulations of various water models *J. Chem. Phys.* **123** 044515
[101] Liu D, Zhang Y, Chen C-C, Mou C-Y, Poole P H and Chen S-H 2007 Observation of the density minimum in deeply supercooled confined water *Proc. Natl Acad. Sci.* **104** 9570–4
[102] Fuentevilla D A and Anisimov M A 2006 Scaled equation of state for supercooled wataer near the liquid–liquid critical point *Phys. Rev. Lett.* **97** 195702
[103] Morishita T 2006 How does tetrahedral structure grow in liquid silicon on supercooling? *Phys. Rev. Lett.* **97** 165502
[104] Xu L, Buldyrev S V, Giovambattista N, Angell C A and Stanley H E 2009 A monatomic system with a liquid–liquid critical point and two distinct glassy states *J. Chem. Phys.* **130** 054505
[105] Sheng H W, Liu H Z, Cheng Y Q, Wen J, Lee P L, Luo W K, Shastri S D and Ma E 2007 Polyamorphism in a metallic glass *Nat. Mater.* **6** 192–7
[106] Bosio L, Teixeira J and Stanley H E 1981 Enhanced density fluctuations in supercooled H_2O, D_2O, and ethanol–water solutions: evidence from small-angle x-ray scattering *Phys. Rev. Lett.* **46** 597–600
[107] Zhang Y, Faraone A, Kamitakahara W A, Liu K-H, Mou C-Y and Chen S-H 2010 Experimental evidence of the existence of a liquid–liquid critical point in supercooled confined water *J. Phys.: Condens. Matter* at press
[108] Banerjee D, Bhat S N, Bhat S V and Leporini D 2009 ESR evidence for two coexisting liquid phases in deeply supercooled bulk water *Proc. Natl Acad. Sci. USA* **106** 11448–53
[109] Mallamace F, Chen S-H, Broccio M, Corsaro C, Crupi V, Majolino D, Venuti V, Baglioni P, Fratini E, Vannucci C and Stanley H E 2007 The role of the solvent in the dynamical transitions of proteins: the case of the lysozyme–water system *J. Chem. Phys.* **127** 045104
[110] Mallamace F, Branca C, Broccio M, Corsaro C, Mou C Y and Chen S H 2007 The anomalous behavior of the density of water in the range 30 K $< T <$ 373 K *Proc. Natl Acad. Sci. USA* **104** 18387–92
[111] Corsaro C, Spooren J, Branca C, Leone N, Broccio M, Kim C, Chen S-H, Stanley H E and Mallamace F 2008 Clustering dynamics in water/methanol mixtures: a nuclear magnetic resonance study at 205 K $< T <$ 295 K *J. Phys. Chem.* B **112** 10449–54
[112] Mallamace F, Corsaro C, Broccio M, Branca C, Gonz'alez-Segredo N, Spooren J, Chen S-H and Stanley H E 2008 NMR evidence of a sharp change in a measure of local order in deeply supercooled confined water *Proc. Natl Acad. Sci. USA* **105** 12725–9
[113] Stanley H E, Buldyrev S V, Canpolat M, Mishima O, Sadr-Lahijany M R, Scala A and Starr F W 2000 The puzzling behavior of water at very low temperature *Phys. Chem. Chem. Phys.* **2** 1551–8
[114] Mishima O and Stanley H E 1998 The relationship between liquid, supercooled and glassy water *Nature* **396** 329–35
[115] Huang C, Wikfeldt K T, Tokushima T, Nordlund D, Harada Y, Bergmann U, Niebuhr M, Weiss T M, Horikawa Y, Leetmaa M, Ljungberg M P, Takahashi O, Lenz A, Ojamäe L, Lyubartsev A P, Shin S, Pettersson L G M and Nilsson A 2009 The inhomogeneous structure of water at ambient conditions *Proc. Natl Acad. Sci. USA* **106** 15214–8
[116] Geiger A and Stanley H E 1982 Low-density patches in the hydrogen-bonded network of liquid water: evidence from molecular dynamics computer simulations *Phys. Rev. Lett.* **49** 1749–52
[117] Geiger A and Stanley H E 1982 Tests of universality of percolation exponents for a 3-dimensional continuum system of interacting waterlike particles *Phys. Rev. Lett.* **49** 1895–8